Adsorption of Cytochrome c on Mesoporous Molecular Sieves: Influence of pH, Pore Diameter, and Aluminum Incorporation

A. Vinu,[†,‡] V. Murugesan,[‡] Oliver Tangermann,[†] and Martin Hartmann*[,†]

Department of Chemistry, Chemical Technology, Kaiserslautern University of Technology, P.O. Box 3049, D-67653 Kaiserslautern, Germany, and Department of Chemistry, Anna University, Chennai 600025, India

Received February 24, 2004. Revised Manuscript Received May 27, 2004

The adsorption of cytochrome c onto different mesoporous molecular sieves (C_{12}−MCM-41, C_{16}−MCM-41 and SBA-15) is studied at different solution pHs. Adsorption isotherms were recorded up to final solution concentrations of ca. 250 μmol/L and were found to be of the pseudo-Langmuir type. Cytochrome c (cyt c) adsorption was observed to be pH-dependent with maximum adsorption near the isoelectric point of the protein. SBA-15 showed a larger amount of cyt c adsorption as compared to MCM-41. The increased cyt c adsorption capacity may be due to the larger pore volume and pore diameter as compared to C_{12}− and C_{16}−MCM-41. It has been discovered that the amount of cyt c adsorption can be increased by the introduction of aluminum into the pure silica materials. The observed increase is most likely a consequence of the strong electrostatic interaction between the negative charges on the aluminum sites and the positively charged amino acid residues of cyt c. Furthermore, the rate of cyt c adsorption has been studied and no significant differences in adsorption rate were found for the mesoporous materials with different pore diameters between 3 and 9 nm. While the adsorption capacity is reduced upon bead formation (due to the reduction in specific pore volume), the rate of adsorption is mainly unchanged.

Introduction

The immobilization of enzymes on inorganic materials is very useful for practical applications because of the potential to improve the stability of enzymes under extreme conditions.[1] Although microporous zeolites and zeotype materials with uniform and molecular-size pores have been widely used as industrial adsorbents, they are not useful in the adsorption of large biomolecules such as proteins, enzymes, or vitamins, owing to their micropore size. Extensive research has been performed on the encapsulation of large biomolecules in sol-gels for possible applications as biosensors and biocatalysts.[2−4] However, sol-gels were found to be unsuitable for the immobilization of large biomolecules due to their broad pore size distribution.[2]

Protein adsorption onto silica and other inorganic matrixes has been reviewed by Weetall[5] and numerous studies of protein adsorption onto silica surfaces are found in the literature.[6−8] Weetall and co-workers[9−13] also used controlled porous glass (CPG) for the immobilization of biological molecules. CPG materials have pore sizes ranging from 30 to 200 nm, which are significantly larger than the biomolecule of interest. Major disadvantages of these materials for adsorption applications are their high cost and more importantly, their low surface area, which rapidly decreases with increasing pore size.[10,13]

The discovery of mesoporous molecular sieves has expanded the available pore sizes of zeolites and zeotypes into the mesopore range, thus opening new possibilities in the adsorption of large molecules such as enzymes and vitamins. Mesoporous materials possess a well-ordered pore structure with high specific surface area and high specific pore volume. SBA-15 is a recently discovered mesoporous silica molecular sieve with uniform tubular channels variable from 5 to 30 nm.[14,15] Several recent papers dealing with the pore structure

* To whom correspondence should be addressed. Phone: +49-631-205-3559. Fax: +49−631-205-4193. E-mail: hartmann@rhrk.uni-kl.de.
† Kaiserslautern University of Technology.
‡ Anna University.

(1) Klibanov, A. M. *Science* **1983**, *219*, 719.
(2) Dave, B. C.; Dunn, B.; Valentine, J. S.; Zink, J. I. *Anal. Chem.* **1994**, *66*, 1120A.
(3) Lan, E. H.; Dave, B. C.; Fukuto, J. M.; Dunn, B.; Zink, J. I.; Valentine, J. S. *J. Mater. Chem.* **1999**, *9*, 45.
(4) (a) Chung, K. E.; Lan, E. H.; Davidson, M. S.; Dunn, B. S.; Valentine, J. S.; Zink, J. I. *Anal. Chem.* **1995**, *67*, 1505. (b) Gill, I.; Ballesteros, A. *J. Am. Chem. Soc.* **1998**, *120*, 8587.
(5) Weetall, H. H. *Appl. Biochem. Biotechnol.* **1993**, *41*, 157.
(6) Docoslis, A.; Wu, W.; Giese, R. F., Van Oss, C. J. *Colloids Surf., B* **1999**, *13*, 83.
(7) Malmsten, M. *J. Colloid Interface Sci.* **1994**, *166*, 333.
(8) Jönsson, U.; Ivarsson, B.; Lundström, I.; Berghem, L. *J. Colloid Interface Sci.* **1982**, *90*, 148.
(9) Weetall, H. H. *Methods Enzymol.* **1976**, *44*, 134.
(10) Weetall, H. H. Vann, W. P.; Pitcher, W. H.; Lee, D. D.; Lee, Y. Y.; Tsao, G. T. *Methods Enzymol.* **1976**, *44*, 776.
(11) Weetall, H. H. Vann, W. P. *Biotechnol. Bioeng.* **1976**, *18*, 105.
(12) Weetall, H. H. *Anal. Chem.* **1974**, *46*, 602A.
(13) Weetall, H. H. *Analytical Uses of Immobilized Biological Compounds for Detection, Medical and Industrial Uses;* Guilbault, G. G., Mascini, M., Eds.; D. Reidel Publishing Co.: Boston; MA, 1988, p 1.
(14) Zhao, D.; Huo, Q.; Feng, J.; Chmelka, B. F.; Stucky, G. D. *J. Am. Chem. Soc.* **1998**, *120*, 6024.

10.1021/cm049718u CCC: $27.50
Published on Web 07/07/2004

of SBA-15,[16,17] assess the possibility of tuning the pore diameter,[18,19] and report the introduction of aluminum.[20] This new class of materials offers the unique opportunity to tailor the pore size of the mesoporous host to accommodate small and large biomolecules by (1) using surfactants with different molecular size, (2) adding of auxiliary organic species during the crystallization process, (3) altering the synthesis temperature, or by (4) suitable postsynthesis hydrothermal treatment.[15,18,19]

Several papers describe the use of mesoporous molecular sieves to immobilize proteins. Balkus et al.[21,22] have studied the immobilization of enzymes with different sizes on MCM-41, MCM-48, and SBA-15. They suggested that the loading efficiency depends on the size of the enzyme and the pore size of the adsorbent, and indicated that the immobilization process takes place in the mesopores. Furthermore, they have found that the proteins retain their activity after adsorption.[22] Takahashi et al.[23] studied the adsorption of horseradish peroxidase and subtilisin on FSM-16, MCM-41, and SBA-15. They found that the amount of adsorption on MCM-41 and FSM-16 is higher as compared to SBA-15. In contrast, Yiu et al.[24] have recently studied the immobilization of trypsin on MCM-41, MCM-48, and SBA-15, and reported that the amount of trypsin adsorbed depends on the pore diameter of the adsorbent and that SBA-15 showed the maximum amount of trypsin adsorption. The separation of biological molecules such as trypsin, lysozyme, and riboflavin has also been performed over MCM-41 and MCM-48 as selective adsorbents.[25] The authors concluded that these adsorbents have advantages over the currently used adsorbents such as bentonite and activated carbon. Stucky et al.[26] have reported the adsorption and release of conalbumin and found that the proteins adsorbed in the mesopores are stable and active. Very recently, Deere et al.[27] reported the adsorption and activity of cytochrome c (cyt c) on mesoporous materials with different pore diameters.[27] They found that cyt c is only adsorbed in the mesopores of MCM-41 with large pore diameter. The peroxidative activity, however, is independent of the pore size of the materials.

Cytochrome c[28,29] is a small heme protein (MW: 12 400 Da) and consists of a single polypeptide chain of 104 amino acid residues that are covalently attached to the heme group. The active heme center consists of a porphyrin ring where the four pyrrole nitrogens are coordinated to the central Fe atom forming a square planar complex. The iron center switches between the ferric (Fe^{3+}) and the ferrous (Fe^{2+}) state, thus acting as a one-electron carrier. Because of the outer electronic structure of Fe^{3+}, it can exist in a high spin or a low spin state. In solution, the iron of cyt c exists in the low spin state at pH between 2 and 12.[30] The heme center is surrounded by tightly packed hydrophobic side chains, a polypeptide chain framework, and an outer covering of hydrophillic side groups. Only one edge of the planar heme ring is accessible to the surface. The cationic side chains of several lysine residues are clustered at the surface of the molecule. Horse heart cyt c is a nearly spherical ($2.6 \times 3.2 \times 3.0$ nm)[31] basic protein with an isoelectric point (pI) of 9.8.[32] The isoelectric point is the pH value in solution at which the sum of the charges on the protein is zero. Some research groups have reported the adsorption of cyt c over various mesoporous molecular sieves.[22,23,27,33−36] However, cyt c adsorption is only studied from low-concentration solutions and the influence of the solution pH and the difference in adsorption behavior of pure silica and aluminum-substituted mesoporous materials have not been studied until now.

In the present contribution, we report the adsorption isotherms of cyt c on MCM-41, AlMCM-41, SBA-15, and AlSBA-15 materials with different pore diameter. The influence of the solution pH on the amount of cyt c adsorption over different adsorbents is also reported. It has been found that the amount of cyt c adsorption on the aluminum-substituted mesoporous adsorbents is higher as compared to their pure silica analogues. Moreover, the amount of cyt c adsorption is maximal near the isoelectric point of the protein. Furthermore, the rate of adsorption onto the powder and the pellet form of the adsorbent is discussed.

Experimental Section

Materials. Horse heart cyt c (90%) was obtained from Acros and used without further purification. For the syntheses of MCM-41 and SBA-15, sodium silicate solution (28.5 wt % SiO_2; 8.5 wt % Na_2O) and tetraethyl orthosilicate from Merck and Aldrich, respectively, were used as silica sources. Sodium aluminate (54 wt % Al_2O_3, 41 wt % Na_2O) and aluminum isopropoxide from Riedel-de-Haën and Merck, respectively, were used as aluminum sources. Alkyltrimethylammonium bromides [$C_nH_{2n+1}(CH_3)_3N$ Br] with $n = 16$ and 12 were obtained from Aldrich and Lancaster, respectively. Triblock copolymer poly(ethylene glycol)-*block*-poly(propylene glycol)-*block*-poly(ethylene glycol) (Pluronic P123, molecular weight = 5800, $EO_{20}PO_{70}EO_{20}$ was obtained from Aldrich.

Syntheses of MCM-41 and AlMCM-41 with Various Pore Diameters. The syntheses of pure siliceous MCM-41

(15) (a) Zhao, D.; Feng, J.; Huo, Q.; Melosh, N.; Fredrikson, G.; Chmelka, B.; Stucky, G. D. *Science* **1998**, 279. (b) Yang, P.; Zhao, D.; Margolese, D.; Chmelka, B.; Stucky, G. D. *Nature* **1998**, *396*, 152.
(16) Miyazawa, K.; Inagaki, S. *Chem. Commun.* **2000**, 2121.
(17) Kruk, M.; Jaroniec, M.; Ko, C. H.; Ryoo, R. *Chem. Mater.* **2000**, *12*, 1961.
(18) Hartmann, M.; Vinu, A. *Langmuir* **2002**, *18*, 8010.
(19) Galarneau, A.; Cambon, H.; Di Renzo, F.; Fajula, F. *Langmuir* **2001**, *17*, 8328.
(20) (a) Luan, Z.; Hartmann, M.; Zhao, D.; Zhou, W.; Kevan, L. *Chem. Mater.* **1999**, *11*, 1621. (b) Yue, Y.; Gedeon, A.; Bonardet, J. L.; Melosh, N.; d'Espinose, J. B.; Fraissard, J. *Chem. Commun.* **1999**, 1967. (c) Gedeon, A.; Lassoued, A.; Bonardet, J. L.; Fraissard, J. *Microporous Mesoporous Mater.* **2001**, *44−45*, 801.
(21) Diaz, J. F.; Balkus, K. J. Jr. *J. Mol. Catal. B: Enzymatic* **1996**, *2*, 115.
(22) Washmon-Kriel, L.; Jimenez, V. L.; Balkus, K. J., Jr. *J. Mol. Catal. B: Enzymatic* **2000**, *10*, 453.
(23) (a) Takahashi, H.; Li, B.; Sasaki, T.; Miyazaki, C.; Kajino, T.; Inagaki, S. *Microporous Mesoporous Mater.* **2001**, *44−45*, 755. (b) Takahashi, H.; Li, B.; Sasaki, T.; Miyazaki, C.; Kajino, T.; Inagaki, S. *Chem. Mater.* **2000**, *12*, 3301.
(24) Yiu, H. H. P.; Wright, P. A.; Botting, N. P. *Microporous Mesoporous Mater.* **2001**, *44−45*, 763.
(25) Kisler, J. M.; Dähler, A.; Stevens, G. W.; O'Connor, A. J. *Microporous Mesoporous Mater.* **2001**, *44−45*, 769.
(26) Han, Y.-J.; Stucky, G. D.; Butler, A. *J. Am. Chem. Soc.* **1999**, *121*, 9897.
(27) Deere, J.; Magner, E.; Wall, J. G.; Hodnett, B. K. *Catal. Lett.* **2003**, *85*, 19.
(28) Harbury, H. A.; Loach, P. A. *J. Biol. Chem.* **1960**, *235*, 3640.
(29) Senn, H.; Wüthrich, K. Q. *Rev. Biophys.* **1985**, *18*, 111.
(30) Scott, R. A.; Mauk, A. G. *Cytochrome c: A multidisciplinary approach*; University of Science Books: Sausalito, CA, 1996.
(31) Guo, L.-H. *Adv. Inorg. Chem.* **1991**, *36*, 341.
(32) Macdonald, I. D. G.; Smith, W. E. *Langmuir* **1996**, *12*, 706.

and aluminum-containing MCM-41 materials with different pore diameters have been performed by variation of the chain length of surfactant as described in the literature.[37] The following gel composition was used for all MCM-41 materials: 10:5.4:4.25:1.3:480 SiO_2:$C_nH_{2n+1}(CH_3)_3NBr$:Na_2O:H_2SO_4:H_2O. A typical synthesis procedure for C_{16}-MCM-41 using hexadecyltrimethylammonium bromide is described below: 34.6 g of hexadecyltrimethylammonium bromide and 115 g of water were mixed and stirred for 30 min. Thereafter, 37.4 g of sodium silicate solution were added dropwise to the surfactant solution under vigorous stirring for another 30 min. Then, 2.4 g of H_2SO_4 in 10 g of water was added to the above mixture and the stirring was continued for another 30 min. The resulting gel was transferred into a polypropylene bottle and kept in an oven at 373 K for 24 h. After cooling to room temperature, the precipitated solid was recovered by filtration, washed with distilled water and dried in an oven at 373 K for 6 h. Finally, the materials were calcined in a muffle furnace at 813 K for 10 h. The synthesis of the AlMCM-41 materials was carried out analogous to the synthesis of MCM-41 and a solution of 0.72 g of sodium aluminate in 5 mL of water was added after addition of the silicon source. The n_{Si}/n_{Al} ratio was fixed at 23, which resulted in the following gel composition: 10:5.4:0.22:3.27:1.3:480 SiO_2:C_nTMABr:Al_2O_3:Na_2O:H_2SO_4:H_2O with n = 12 and 16. The pure silica samples are denoted as C_n−MCM-41 and the aluminum-substituted forms are denoted as C_n−AlMCM-41, where n indicates the number of the carbon atoms of the alkyl side chain of the surfactant which was employed in the synthesis.

Syntheses of SBA-15 and AlSBA-15. SBA-15 was synthesized using the tri-block copolymer poly(ethylene glycol)-*block*-poly(propylene glycol)-*block*-poly(ethylene glycol) (Pluronic P123, Molecular weight = 5800, $EO_{20}PO_{70}EO_{20}$) as a structure-directing agent according to the method reported in the literature.[18] In a typical synthesis, 4 g of Pluronic P123 was added to 30 mL of water. After stirring for a few hours, a clear solution was obtained. Thereafter, 120 mL of 2 M HCl was added and the solution was stirred for another 2 h. Then, 9 g of tetraethyl orthosilicate was added and the resulting mixture was stirred for 24 h at 313 K, and subsequently heated for 48 h to 373 K. The solid product was recovered by filtration, washed several times with water, and dried overnight at 373 K. Finally, the product was calcined at 813 K to remove the template. The synthesis of AlSBA-15 was carried out analogous to the synthesis of the SBA-15 with the slight modification of adding 70 mL of 0.29 M HCl instead of adding 120 mL of 2M HCl. Moreover, aluminum isopropoxide was added after the addition of the silicon source. In a second set of experiments, the synthesis temperature was varied from 373 to 403 K in order to synthesize SBA-15 materials with different textural properties.[18]

Characterization. The X-ray powder diffraction patterns were recorded on a Siemens D5005 diffractometer using Cu Kα radiation. Nitrogen adsorption and desorption isotherms were measured at 77 K on a Quantachrome Autosorb 1 sorption analyzer. The parent materials were outgassed at 513 K for 3 h prior to the adsorption measurements, while the enzyme-loaded samples were outgassed at 40 °C for 24 h. The specific surface area was determined using the standard Brunauer−Emmett−Teller (BET) method, while the pore size distribution was calculated using the Nonlocal Density Functional Theory (NLDFT). To obtain MCM-41 and SBA-15 pellets, the calcined samples were compressed in a steel die of 24-mm diameter, using a hand-operated press, for 30 min. The two external pressures applied (43 and 108 MPa) were calculated from the external force applied and the diameter of the die. The pressed samples were denoted as C_n−MCM-41(p) and SBA-15(p), where p specifies the pressure in MPa. Subsequently, the obtained disk was crushed and sieved to obtain pellets with a diameter of 0.2 to 0.35 μm.

Table 1. Textural Parameters of the Pure Silica and Aluminum-Substituted MCM-41 Materials

sample	pelletizing pressure/ (MPa)	a_0/ (nm)	A_{BET}/ (m^2/g)	pore volume/ (cm^3/g)	$d_{p,NLDFT}$/ (nm)
C_{12}−AlMCM-41	0	3.47	1024	0.57	3.2
C_{12}−MCM-41	0	3.54	1212	0.70	3.1
C_{12}−MCM-41(43)	43	3.62	1109	0.63	3.1
C_{12}−MCM-41(107)	107	3.61	1057	0.59	3.1
C_{16}−AlMCM-41	0	4.15	1105	0.79	3.8
C_{16}−MCM-41	0	4.10	1135	0.86	3.9
C_{16}−MCM-41(43)	43	4.37	993	0.74	3.9
C_{16}−MCM-41(107)	107	4.25	962	0.69	3.9

Cytochrome c Adsorption. A series of standard cyt c solutions with concentrations ranging from 0.25 to 4.0 g/L was prepared by dissolving different amounts of cyt c in 25 mM buffer solutions (pH = 3 citric acid buffer, pH = 6.5 and 8.0 potassium phosphate buffer, pH = 9.6 and 10.6 sodium bicarbonate buffer). In each adsorption experiment, 20 mg of the different mesoporous adsorbents were suspended in 4 g of the respective cyt c solution. The resulting mixture was continuously shaken in a shaking bath with the speed of 160 shakes/minute at 293 K until equilibrium was reached (typically 72−96 h). The amount of cyt c adsorbed was calculated by subtracting the amount found in the supernatant liquid after adsorption from the amount of cyt c present before addition of the adsorbent by UV absorption at 409 nm. Calibration experiments were done separately before each set of measurements with cytochrome c solutions of different concentrations buffered at the pH of the isotherm measurement. UV−Vis spectra of the cytochrome c solution before and after the adsorption experiments were recorded to ensure that the changes in the intensity of the 409 nm absorption band (Soret band) are solely due to the change of cyt c concentration. Centrifugation prior to the analysis was used to avoid potential interference from scattering particles in the UV−Vis analysis. For the kinetic experiments, 20 mg of the powdered or the pelletized form of a mesoporous adsorbent (only pure silica materials) were suspended in 4 g of a cyt c (concentration c = 1 g/L) solution for each measurement, and the solutions were analyzed every 2 h until thermodynamic equilibrium was reached.

Results and Discussion

Characterization. The powder XRD patterns reveal that all mesoporous adsorbents employed in the present study show higher-order reflections that are characteristic of high quality C_n−MCM-41 and SBA-15 silicas (Figure S1, Supporting Information). Nitrogen adsorption isotherms and pore size distributions (calculated using the NLDFT method) of C_n−MCM-41 and C_n−AlMCM-41 are shown in Figures S2 and S3 (see Supporting Information), respectively. Textural properties of the pressed and unpressed form of pure silica and aluminum-substituted C_n−AlMCM-41 materials are collected in Table 1. All materials under investigation possess a surface area of around 1000 m^2/g and the pore diameter exceeds 3.0 nm (calculated using NLDFT), which is larger than the molecular diameter of cyt c. The adsorption isotherms of the MCM-41 samples are of type IV of the IUPAC classification featuring a region of capillary condensation that provides clear evidence for their narrow pore size distribution (Figure S3). Textural parameters of pure silica SBA-15 and its

(33) Deere, J.; Magner, E.; Wall, J. G.; Hodnett, B. K. *Chem. Commun.* **2001**, 465.
(34) Deere, J.; Magner, E.; Wall, J. G.; Hodnett, B. K. *J. Phys. Chem. B* **2002**, *106*, 7340.
(35) Yiu, H. H. P.; Botting, C. H.; Botting, N. P.; Wright, P. A. *Phys. Chem. Chem. Phys.* **2001**, *3*, 2983.
(36) Gimon-Kinsel, M. E.; Jimenez, V. L.; Washmon, L.; Balkus, K. J., Jr. *Stud. Surf. Sci. Catal.* **1998**, *117*, 373.
(37) Hartmann, M.; Raccouchot, S.; Bischof, C. *Microporous Mesoporous Mater.* **1999**, *27*, 309.

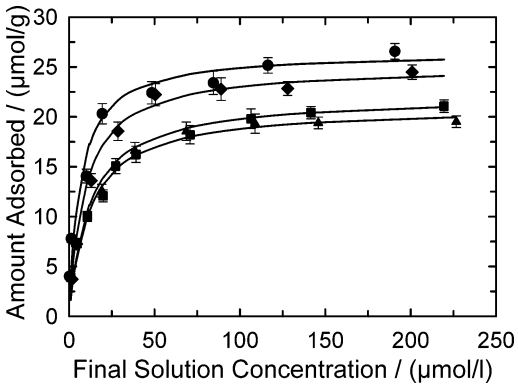

Figure 1. Adsorption isotherms at 293 K of cyt c on C_{16}−MCM-41 at various solution pHs: (▲) pH = 3.0, (■) pH = 6.5, (●) pH = 9.6, and (◆) pH = 10.6. By repeating single experiments up to 10 times, the standard deviation has been found to be below 5% for initial concentrations up to 2 g/L and below 3% above 2 g/L, which is indicated by the error bars.

Table 2. Textural Parameters and Synthesis Conditions of the Pure Silica and Aluminum-Substituted SBA-15 Materials

sample	synthesis temperature/ (°C)	a_0/ (nm)	A_{BET}/ (m^2/g)	pore volume/ (cm^3/g)	$d_{p,NLDFT}$/ (nm)
SBA-15	100	10.89	910	1.25	8.8
SBA15-100	120	10.52	883	1.27	9.1
SBA-15-130	130	10.54	546	1.19	9.8
SBA-15-150	150	10.83	393	1.10	11.2
SBA-15(43)	100	10.52	757	0.99	8.1
SBA-15(107)	100	10.42	699	0.92	8.1
AlSBA-15	100	11.64	930	1.35	9.1

aluminum-substituted analogue are collected in Table 2. It is interesting to note that the pore diameter of pure silica SBA-15 increases with synthesis temperature at the expense of specific pore volume and surface area.[18]

Influence of pH on Cyt c Adsorption. Adsorption isotherms of cyt c adsorbed onto C_{16}−MCM-41 at different solution pHs ranging from 3.0 to 10.6 are shown in Figure 1. Cyt c is not stable and denatured at pH below 3.0 and above 11; therefore, the adsorption was not studied outside this pH range. Each isotherm shows a sharp initial rise, suggesting a high affinity between cyt c and the adsorbent surface. Finally, the isotherm reaches a plateau and thus, the isotherms are of Type L (pseudo-Langmuir isotherm). The solid lines in this figure represent a fit of the experimental data employing the Langmuir model. The monolayer adsorption capacity was calculated by using the Langmuir equation

$$n_s = Kn_m c/(1 + Kc)$$

where K is the Langmuir constant, c is the concentration of cyt c, n_m is the monolayer adsorption capacity, and n_s is the amount of cyt c adsorbed on the adsorbent.

The isoelectric point (pI) of cyt c is 9.8, and hence, the protein is positively charged at a pH below pI and negatively charged at a pH above pI. The isoelectric point (or better, the point of zero charge PZC) of the silica surface of the mesoporous materials is around 2;[38] hence, the adsorbent surface is negatively charged at a pH above 2. The candidates for the dominant driving forces for the adsorption of cyt c include hydrophobic interactions (a kind of van der Waals attraction), electrostatic repulsion and attraction between the amino acid residues on the surface of cyt c and silanol groups on the surface of the silica walls of the mesoporous materials, the intramolecular cohesive attraction and repulsion and, thus, expansion and contraction of the molecular diameter of cyt c at different pH.[39] It can be clearly seen from the Figure 2 that the amount of adsorption is significantly affected by the solution pH. The amount adsorbed increases from pH 3.0 to pH 9.6 and decreases from pH 9.6 to pH 10.6. The maximum adsorption of cyt c amounts to 26.6 μmol/g at a pH of 9.6, while only 19.8 μmol/g are adsorbed at pH 3.0. The maximal loading is clearly a function of solution pH, which is in some disagreement with the results of Diaz and Balkus[21] who reported that cyt c adsorption on MCM-41 was less susceptible to pH changes of the solution. If the pH of the solution is lower than the pI of cyt c, the positively charged lysine and histidine residues at the surface of cyt c interact with the various partially negatively charged surface groups of the adsorbent such as isolated, hydrogen-bonded, and geminal silanol groups of the silica framework of the adsorbent. With decreasing pH, the net positive charge of the protein increases and repulsive Coulombic forces between the amino acid residues occur. As a consequence, the protein molecules require more space and the monolayer capacity decreases.

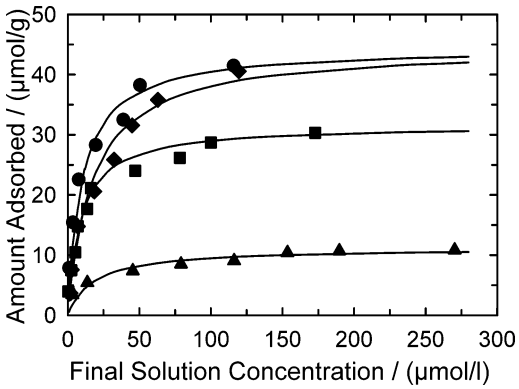

Figure 2. Adsorption isotherms at 293 K of cyt c on SBA-15 at various solution pHs: (▲) pH = 3.0, (■) pH = 6.5, (●) pH = 9.6, and (◆) pH = 10.6.

Figure 1 shows that the amount adsorbed is maximal at pH 9.6, which is close to the pI of cyt c (9.8). Under these conditions, the net charge of the protein is low and the Coulombic repulsive force between the protein molecules is minimal. Consequently, closer packing of the protein molecules is possible and the monolayer capacity increases. Near the isoelectric point, the binding to the surface of MCM-41 can be considered analogous to a neutralized precipitation between the cyt c molecules and the adsorbent. Thus, the Coulombic forces derived from the positive charges of the ionized proteins and the negative charges at the surface of the adsorbent are small. Under these circumstances, the hydrophobic interaction between the protein and the adsorbent become more important. (Hydrophobic inter-

(38) Iler, R. K. *The Chemistry of Silica*; John Wiley & Sons: New York, 1979.

(39) Matsui, M.; Kiyozumi, Y.; Yamamoto, T.; Mizushina, Y.; Mizukami, F.; Sakaguchi, K. *Chem. Eur. J.* **2001**, *7*, 1555.

actions are believed to be much weaker (by about 1/13 in water) than Coulombic forces.)[39] These hydrophobic interactions may either originate from attraction of the nonpolar side chains of the amino acids residues on the surface of cyt c by siloxane bridges at the adsorbent surface or from cyt c−cyt c interactions between the hydrophobic side chains of neighboring cyt c molecules adsorbed on the surface of MCM-41. It should be noted that the surface structure of the adsorbent (i.e., in the mesopores) is very important when adsorption occurs mainly by hydrophobic interactions.

At a solution pH larger than the isoelectric point, the amount of cyt c adsorbed is reduced. The cyt c molecule is negatively charged at this pH (10.6), and thus, the electrostatic repulsion between the negatively charged cyt c molecules and the negatively charged silanol groups of the adsorbent results in a reduced amount of adsorption.

The adsorption isotherms of cyt c on SBA-15 at various solution pHs are shown in Figure 2. The amount of cyt c adsorbed increases with pH up to 9.6 and declines at pH 10.6. A maximum amount adsorbed of 41.5 μmol/g is obtained at pH 9.6. It is interesting to note that the adsorption of cyt c on SBA-15 shows the same trend as observed for C_{16}−MCM-41 except for the experiment at pH 10.6, which is above the pI of cyt c. Here, the adsorption capacity is close to that found at pH 9.6. It is surmised that the increase in the diameter of the cyt c molecule due to the electrostatic repulsion between the negative carboxyl groups does not influence the amount of adsorption since the adsorbent pore diameter is more than two times higher than the size of the cyt c molecule. Moreover, the surface curvature of the SBA-15 pores is larger as compared to C_{16}−MCM-41, and, therefore, the electrostatic repulsion between the carboxyl groups of neighboring adsorbate complexes that are sited on the walls of the adsorbent might be reduced. It should also be noted that at pH 3.0 the amount of cyt c adsorbed (10.4 μmol/g) is very low compared to C_{16}−MCM-41 at the same pH (19.8 μmol/g), which is tentatively assigned to (partial) denaturation of the protein in SBA-15 at this pH. However, further studies are underway to study the structural changes of the protein adsorbed on different supports.

Adsorption isotherms of cyt c on MCM-41 and SBA-15 at pH = 6.5 have been reported by Deere et al.[27,33,34] up to an equilibrium concentration of 10 μmol/L. At this concentration, the amount adsorbed corresponds to 1, 8, and 6.8 μmol/g for MCM-41 (d_p = 2.8 nm), MCM-41 (d_p = 4.5 nm), and SBA-15, respectively. This is in line with our results at this equilibrium concentration, although we have found that the use of higher-concentrated cyt c solutions allows the adsorption of higher quantities of cyt c. This shows that Deere et al.[34] only recorded the initial part of the isotherm and that saturation was probably not reached in their experiments. The authors therefore concluded that cyt c is not entering the mesopores of MCM-41 (d_p = 2.8 nm), while our data clearly show that cyt c is adsorbed in the mesopores of C_{12}−MCM-41, which has a pore diameter of ca. 3.0 nm (NLDFT method). Moreover the pore volume of their material is very low (0.31 cm^3/g for MCM-41 (d_p = 2.8 nm) which also accounts for the low adsorption capacity observed. In a more recent paper by the same authors, an adsorption capacity of 8 μmol/g was found for a MCM-41 sample with a higher pore diameter of 4.5 nm.[27] Balkus et al.[21,22] studied the adsorption of cyt c at 0 °C and pH = 7 onto MCM-41, MCM-48, and SBA-15. The maximum adsorption reported was around 7 μmol/g starting from solution concentrations of 15 μmol/L which is well below the final concentration used in this study (ca. 320 μmol/L).

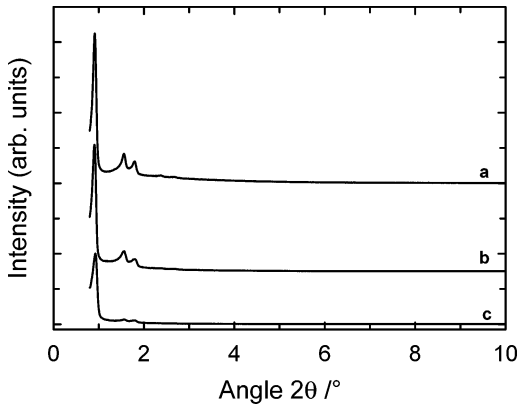

Figure 3. XRD powder patterns of SBA-15 before and after cyt c adsorption at pH 9.6 (time of exposure: 72 h): (a) SBA-15, (b) SBA-15 (1 g/L*), (c) SBA-15 (4 g/L*). *Initial concentration of cyt c.

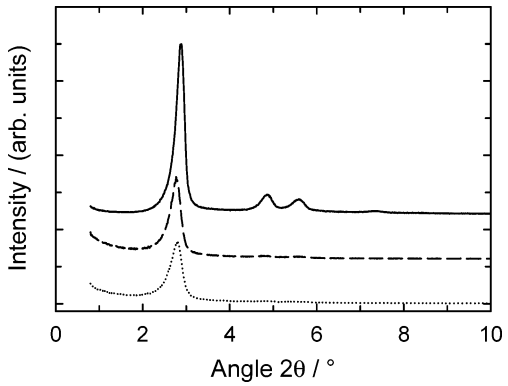

Figure 4. XRD powder patterns of C_{12}−MCM-41 before and after cyt c adsorption at pH 9.6 (time of exposure: 72 h): (a) C_{12}−MCM-41, (b) C_{12}−MCM-41 (1 g/L*), (c) C_{12}−MCM-41 (4 g/L*). *Initial concentration of cyt c.

To answer the question of whether cyt c enters the mesopores of MCM-41 and SBA-15, all materials were also characterized by XRD and nitrogen adsorption after protein adsorption. The powder XRD patterns of SBA-15 and C_{12}−MCM-41 before and after the adsorption experiment (72 h) at two different initial cyt c concentrations (1 and 4 g/L) at pH 9.6 are shown in Figure 3 and Figure 4, respectively. All samples exhibit XRD patterns typically observed for SBA-15 and C_{12}−MCM-41, respectively, consisting of a strong (100) reflection at low angle and two small peaks at higher angle. The observation of these peaks even after loading the sample at a pH of 9.6 with ca. 41.5 μmol/g of cyt c (duration of the adsorption experiment: 72 h) confirms retention of the hexagonal mesoporous structure. As explained above, the amount adsorbed increases with the initial cyt c concentration. With increasing initial concentration of the cyt c solution, the intensity of the low angle (100) and high angle peaks (110 and 200) decreases as compared to the parent SBA-15 and C_{12}−MCM-41

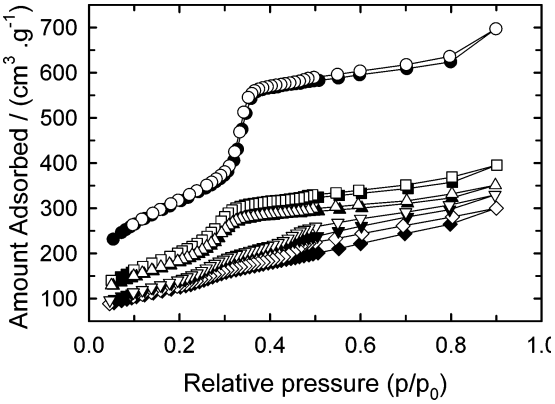

Figure 5. Nitrogen adsorption isotherms C_{16}−MCM-41 after cyt c adsorption (time of exposure: 72 h) at various pHs (initial concentration 1 g/L): (●) C_{16}−MCM-41 (before adsorption), (■) pH = 3.0, (▲) pH = 6.5, (▼) pH = 9.6, and (◆) pH = 10.6.

materials. This is probably due to the larger contrast in density between the silica walls and the empty pores relative to that between the silica walls and the pores filled with cyt c molecules.[40] This effect is more pronounced when a higher cyt c loading was achieved. XRD patterns of the pure silica SBA-15 and C_{16}−MCM-41 adsorbents after the adsorption of cyt c at different solution pHs are shown in Figures S4 and S5 (see Supporting Information), respectively. Retention of the structure of all SBA-15 mesoporous adsorbents after cyt c adsorption at different solution pHs is indicated by the XRD patterns observed. Moreover, the reduction in the intensity of the XRD reflections of SBA-15 at different solution pHs is directly related to the amount of cyt c adsorption at different solution pHs. This supports the conclusion that cyt c molecules can be packed inside the mesopores without affecting the structural integrity of the adsorbent. In the case of C_{16}−MCM-41 (similarly for SBA-15 and C_{12}−MCM-41), the intensity of the XRD peaks also decreases with increasing pH of the solution. However, the reduction in the intensity of XRD peaks at a solution pH of 10.5 is higher as compared to that observed at a pH of 9.6. This loss in intensity cannot solely be ascribed to the adsorption of cyt c in the mesopores, but it is likely that the reduced intensity of XRD reflection after adsorption at this pH indicates a loss of structural order. Nitrogen adsorption isotherms of C_{16}−MCM-41 recorded after the adsorption of cyt c at different solution pH are shown in Figure 5. The amount of nitrogen adsorbed decreases with increasing pH of the solution, which is in line with the amount of cytochrome c adsorbed. This gives additional evidence for the adsorption of cyt c in the mesopores of C_{16}−MCM-41. However, the amount of nitrogen adsorbed after cyt c adsorption at pH 10.5 is lower compared to that obtained at a pH of 9.6 although the amount of cyt c adsorbed is lower. Therefore, from the XRD patterns and the nitrogen adsorption data we have to assume that some loss of structural order occurs at this solution pH.

N_2 adsorption isotherms of SBA-15 and C_{12}−MCM-41 before and after loading with different amounts of cyt c (initial concentrations of 1 and 4 g/L) are shown

(40) Marler, B.; Oberhagemann, U.; Vortmann, S.; Gies, H. *Microporous Mesoporous Mater.* **1996**, *6*, 375.

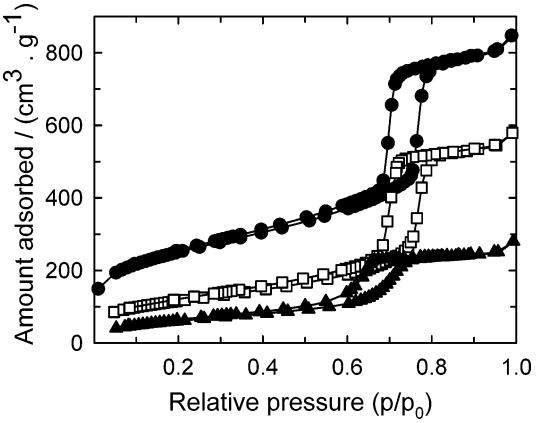

Figure 6. Nitrogen adsorption isotherms of SBA-15 before and after cyt c adsorption (time of exposure: 72 h) at pH 9.6: (open symbols: Adsorption; closed symbols: desorption): (●) SBA-15, (□) SBA-15(1 g/L), (▲) SBA-15(4 g/L).

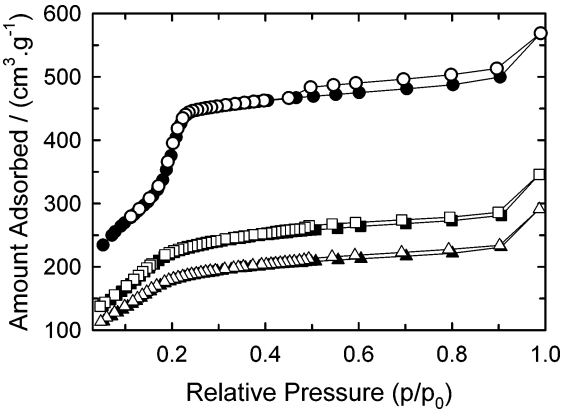

Figure 7. Nitrogen adsorption isotherms of C_{12}−MCM-41 before and after cyt c adsorption at pH 9.6 (time of exposure: 72 h): (closed symbols: Adsorption; open symbols: desorption): (●) C_{12}−MCM-41, (□) C_{12}−MCM-41(1 g/L), (▲) C_{12}−MCM-41(4 g/L).

Table 3. Amount of Cytochrome c Adsorbed at pH = 9.6 onto Different Mesoporous Materials and by Adsorbed Cytochrome c Occupied Volume

sample	Cyt c adsorbed/ (μmol/g)	volume occupied $V_{cyt\ c}$/(cm^3/g)	V_p/(cm^3/g)	$V_{cyt\ c}/V_p$/%
C_{12}−MCM-41	12.2	0.10	0.70	14
C_{16}−MCM-41	26.5	0.23	0.86	27
SBA-15	41.5	0.35	1.25	28
C_{12}−AlMCM-41	17.7	0.15	0.57	26
C_{16}−AlMCM-41	30.7	0.26	0.79	32
AlSBA-15	37.0	0.31	1.35	23

in Figure 6 and Figure 7, respectively. It is observed that the amount of nitrogen adsorbed decreases with increasing cyt c loading. The pore volume of SBA-15 decreases from 1.25 to 0.39 cm^3/g, whereas the surface area is reduced from 930 to 233 m^2/g upon adsorption of the protein. Assuming that cyt c is a spherical protein with a diameter of 3 nm, the volume occupied by the protein is calculated to 14.3 nm^3. Therefore, the adsorption of 41.5 μmol/g of cyt c corresponds to an occupied volume of 0.35 cm^3/g (Table 3). Thus, it is shown that such a quantity of cyt c can be accommodated in the mesopores of SBA-15. The observed decrease in pore volume of ca. 0.86 cm^3/g of SBA-15 after loading with 41.5 μmol/g cyt c cannot be attributed to the adsorption of cyt c alone. It is, however, well accepted that SBA-15

Table 4. Specific Surface Areas A_{BET} and Specific Pore Volumes V_p of the Silica and Aluminum-Substituted Mesoporous Materials before and after Cytochrome c Adsorption at pH 9.6

	before adsorption		after adsorption ($c_{cyt\ c}$ = 1 g/L)		after adsorption ($c_{cyt\ c}$ = 4 g/L)	
sample	A_{BET}/ (m^2/g)	V_p/ (cm^3/g)	A_{BET}/ (m^2/g)	V_p/ (cm^3/g)	A_{BET}/ (m^2/g)	V_p/ (cm^3/g)
C_{12}−MCM-41	1212	0.70	733	0.37	613	0.30
C_{16}−MCM-41	1135	0.86	458	0.28	358	0.20
SBA-15	910	1.25	505	0.84	233	0.39
C_{12}−AlM CM-41	1024	0.57	574	0.31	199	0.10
C_{16}−AlM CM-41	1105	0.79	435	0.26	303	0.17
AlSBA-15	930	1.35	419	0.92	208	0.39

possesses a large quantity of (ultra)micropores,[18,41,42] which can account for up to 50% of the measured pore volume. We, therefore, assume that some of the cyt c molecules also block the pore mouth of the (ultra)-micropores present in the SBA-15 silica walls. Hence, those micropores are not accessible for nitrogen, resulting in a large reduction of the pore volume after cyt c adsorption. The reduction in the amount of nitrogen adsorbed after the adsorption of different amounts of cyt c on C_{12}−MCM-41 indicates that cyt c is adsorbed inside the pores of C_{12}−MCM-41 (Figure 7). Similar results have been obtained for other adsorbents such as C_{16}−MCM-41 and C_{16}−AlMCM-41 after cyt c adsorption. Table 4 summarizes the textural properties of pure silica and aluminum-substituted mesoporous samples before and after loading with the different amounts of cyt c (initial concentration of 1 and 4 g/L initial concentration) at pH 9.6. The specific surface area and the specific pore volume of all the samples are reduced after cyt c adsorption. The large reduction in the specific pore volume and the specific surface area are tentatively attributed to the tight packing of cyt c molecules in the pores of mesoporous materials. It is interesting to note that the reduction of the specific surface area and the pore volume of C_{12}−MCM-41 after different loadings of cyt c adsorption is less as compared to other mesoporous materials. This shows that part of the C_{12}−MCM-41 pores is too small to be accessible for cytochrome c.

UV−Vis spectra of the cyt c solution before the adsorption and the supernatant cyt c solution of C_{16}−MCM-41 and C_{16}−AlMCM-41 after the 72 h of adsorption are shown in Figure 8. All three spectra show a maximum at ca. 409 nm (Soret band). Moreover, it should be noted that the intensity ratio of the Soret band and the band at 365 nm does not change during the adsorption experiments, indicating that unfolding of the protein does not occur. However, in the UV−Vis DRS spectrum of cyt c adsorbed on C_{16}−MCM-41 and C_{16}−AlMCM-41, the maximum of the Soret band is shifted to ca. 406 nm and the peaks are somewhat broader compared to those of the liquid samples (not shown). The stability of cyt c during the adsorption was also confirmed by Raman spectroscopy in an independent study.[34]

Influence of Aluminum. The adsorption isotherms of cyt c on aluminum-substituted C_{16}−AlMCM-41 at various pHs are shown in Figure 9. It is interesting to note that the amount of cyt c adsorbed on aluminum-substituted C_{16}−MCM-41 adsorbents decreases from 31.2 μmol/g at pH 9.6 to 21.9 at pH 10.6 (Figure 9). As explained above, the protein net charge approaches zero near its pI, and thus the intermolecular interactions are reduced and, hence, an adsorbed cyt c molecule requires less space on the adsorbent surface and allows denser packing of cyt c. Moreover, the reduced amount of adsorption at pH 10.6 is attributed to the strong electrostatic repulsion between the cyt c molecule and the adsorbent surface. This is evident from the monolayer adsorption capacity, which is increased from 24.0 to 31.2 μmol/g for the pH range 3.0−9.6 and decreased to 21.9 μmol/g for a pH of 10.6.

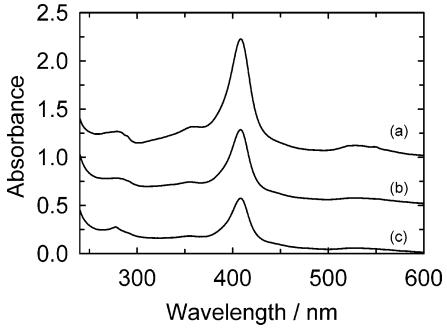

Figure 8. UV−vis spectra of a (a) cyt c solution (c = 0.25 g/L) before and after adsorption experiments with (b) C_{16}−AlMCM-41 and (c) C_{16}−MCM-41 at pH = 9.6.

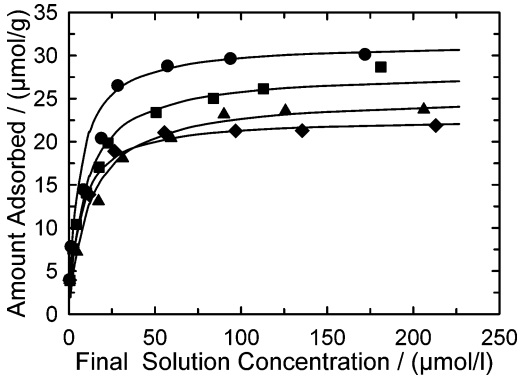

Figure 9. Adsorption isotherms at 293 K of cyt c on C_{16}−AlMCM-41 at various solution pH: (▲) pH = 3.0, (■) pH = 6.5, (●) pH = 9.6, and (◆) pH = 10.6.

In Figure 10, the monolayer adsorption capacities of pure silica C_{16}−MCM-41 and C_{16}−AlMCM-41 are compared as a function of solution pH. The amount of cyt c adsorbed is larger as compared to all-silica C_{16}−MCM-41 at all pH studied except at pH 10.6. The difference in adsorption is more pronounced at lower pH. Two reasons might account for this behavior: first, at lower pH, the positively charged amino acid residues on the surface of the cyt c can interact both with the surface silanol groups and the negatively charged aluminum sites on the surface of the adsorbent, resulting in a stronger interaction; second, there are two areas of positive charges that can most effectively bind to a negatively charged surface at lower pH. One region is the lysine-rich surface (Lys-54, Lys-55, Lys-72, Lys-73, and His-39), while the other has surface residues of histidine and lysine (His-33, His-36, Lys-22, and Lys-27).[32] Both regions could compete for adsorption sites,

(41) Galarneau, A.; Cambon, H.; Di Renzo, F.; Ryoo, R.; Choi, M.; Fajula, F. *New J. Chem.* **2003**, *27*, 73.
(42) Van der Voort, P.; Ravikovitch, P. I.; De Jong, K. P.; Mejelloun, M.; Van Bavel, E.; Janssen, A. H.; Neimark, A. V.; Weckhuysen, B. M.; Vansant, E. F. *J. Phys. Chem. B* **2002**, *106*, 5873.

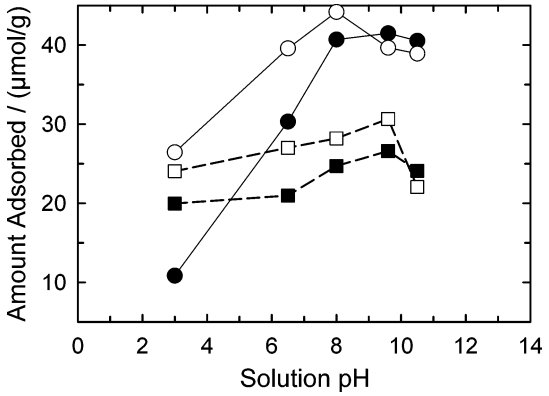

Figure 10. Monolayer capacities of (○) AlSBA-15, (●) SBA-15, (□) C_{16}−AlMCM-41, and (■) C_{16}−MCM-41 as a function of the solution pH.

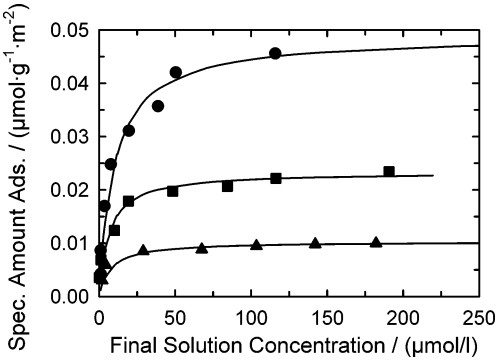

Figure 11. Comparison of the area-specific cyt c adsorption isotherms on mesoporous adsorbents with various pore diameters at pH 9.6: (●) SBA-15, (■) C_{16}−MCM-41, and (▲) C_{12}−MCM-41.

and interact strongly with both the negative charges of the surface silanol groups and aluminum atoms. Raising the pH will deprotonate the histidine residues on the surface of cyt c because the isoelectric point of histidine is 7.6. Therefore, the electrostatic interaction with the surface of the adsorbent will be reduced and only a smaller difference between the pure silica and aluminum-substituted analogues is observed at higher pH. A similar increase in adsorption capacity at pH 3 to 6.5 upon introduction of aluminum is found for C_{12}−AlMCM-41 (Table 3). For AlSBA-15, the adsorption capacity is higher as compared to SBA-15 at pH 3 and 6.5, while it is slightly lower at a pH of 9.6 (Figure 10). It has been reported by Haynes and Norde[43] that the maximal amount adsorbed peaks at the isoelectric point of the protein/substrate complex and not at the pI of the bulk solution. The reason for low adsorption of AlSBA-15 at pH 9.6 is that on contact the negative charges on the adsorbent surface neutralize some of the positively charged groups on the protein, causing a shift of the bulk solution isoelectric point to a lower pH. The increase in the number of negative charges on the surface of AlSBA-15 due to the higher number of Al atoms might shift the pI of the cyt c solution to a lower pH, which results in an increase in the number of positive charges on the surface of the protein. Hence, we decided to study the adsorption of cyt c over AlSBA-15 and other mesoporous materials at the solution pH 8.0. It is interesting to note that AlSBA-15 shows the maximal adsorption of 44.2 μmol/g, which is the highest cyt c amount adsorbed in this study. Whereas, other mesoporous materials such as C_{12}−MCM-41, C_{16}−MCM-41, C_{16}−AlMCM-41, and SBA-15 show a lower amount of adsorption at this pH compared to the amount of adsorption at the pH 9.6. Thus, we surmised that the low adsorption capacity of AlSBA-15 at pH 9.6 and higher amount of adsorption at pH 8.0 in AlSBA-15 could be due to the shift of the pI of the cyt c solution from 9.8 to lower pH. The same behavior has also been seen by Haynes and Norde et al.[43] in the adsorption of lysozyme. Detailed studies on the variation of the amount of cyt c adsorption as a function of the number of aluminum atoms in the mesoporous materials are underway.

Moreover, it is also interesting to note that the amount adsorbed on C_{16}−MCM-41 (24.5 μmol/g) is higher than on C_{16}−AlMCM-41 (21.9 μmol/g) at pH = 10.6. The electrostatic repulsion between the negative carboxyl species of cyt c and the negative charges on the surface of C_{16}−AlMCM-41 is stronger as compared to the pure silica materials C_{16}−MCM-41, where the repulsion is due to the silanol groups. This agrees very well with the observed reduction of the amount of adsorption.

Influence of Pore Diameter and Pore Volume. Figure 11 compares the adsorption isotherms of cyt c on pure silica mesoporous adsorbents such as C_{12}−MCM-41 and C_{16}−MCM-41 in comparison to the large pore material SBA-15 at pH 9.6. To account for the different surface areas of the samples, the amount adsorbed was divided by the specific surface area of the adsorbent. The area-specific adsorption capacity increases in the following order: C_{12}−MCM-41 < C_{16}−MCM-41 < SBA-15, while the specific surface area decreases in the same order (Tables 1 and 2). Moreover, it should be noted that the area-specific amount of cyt c adsorbed of aluminum-substituted materials is higher than that of the corresponding pure silica materials. (Figure 12). This confirms that the introduction of aluminum results in an enhanced adsorption of cyt c irrespective of the pore diameter.

It is interesting to note that the total volumes occupied by cyt c molecules are only 13.7, 26.4, and 28.3% of the total free volume of C_{12}−MCM-41, C_{16}−MCM-41, and SBA-15 adsorbents (Table 3), respectively. Specific pore volume, specific surface area, and pore diameter are quite different for the three materials compared here (Table 2). Pore volume and pore diameter of C_{12}−MCM-41 are significantly lower as compared to C_{16}−MCM-41. The molecular diameter of cyt c (ca. 3.0 nm) is in the range of the pore size of C_{12}−MCM-41. Thus, the diffusion into the pore may be hindered. Those pores that have pore diameters below 3.0 nm might not be accessible to cyt c molecules and, hence, a reduced adsorption capacity is expected. In an earlier study,[34] it was concluded that cyt c adsorption occurs exclusively at the outer surface of MCM-41 with a pore diameter of 2.8 nm (determined from the nitrogen adsorption isotherm using the BJH method, which typically underestimates the pore size by ca. 1 nm). However, such a behavior was not observed for our MCM-41 samples.

The observed high adsorption capacity for SBA-15 is probably a consequence of its large pore volume and pore diameter. Moreover, the density of the surface

(43) Hayns, C. A.; Norde, W. *Colloids Surf., B* **1994**, *2*, 517.

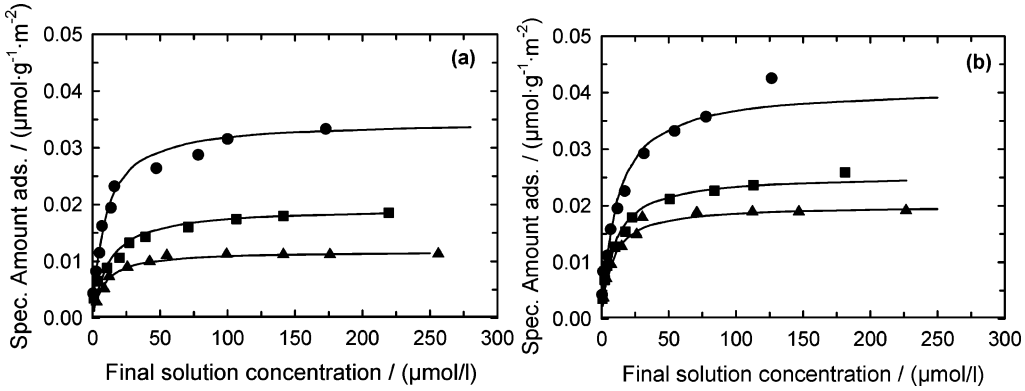

Figure 12. Comparison of the area-specific cyt c adsorption isotherms on mesoporous silica (a) and aluminosilicate (b) adsorbents with various pore diameters at pH 6.5: (●) (Al)SBA-15, (■) C_{16}−(Al)MCM-41, and (▲) C_{12}−(Al)MCM-41.

silanol groups could also play an important role. Recently, Munsch[44] has reported that the surface hydroxyl density of fully hydrated SBA-15 (4.9 OH groups per nm^2) is higher than that of C_{16}−MCM-41 (4.1 OH groups per nm^2). These hydroxyl groups are responsible for the electrostatic interactions that enhance the amount of adsorption. However, it is interesting to note that almost the same fraction of the total pore volume is occupied by cyt c molecules in C_{16}−MCM-41 as compared to SBA-15 (Table 3). Therefore, a plausible working hypothesis is that an increase in specific pore volume is needed to further increase the adsorption capacity.

To check whether the increase of the amount of cyt c adsorption from C_{12}−MCM-41 to SBA-15 is due to the pore diameter or the specific pore volume mesoporous materials, we studied the cyt c adsorption over large pore diameters of SBA-15 with different specific pore volume and pore diameter. Recently, we have reported the synthesis of SBA-15 at different temperatures resulting in an increase of the pore diameter of SBA-15 at the expense of specific pore volume and specific surface area.[18] The samples are denoted as SBA-15-x where x indicates the synthesis temperature. The adsorption isotherms of cyt c on pure silica SBA-15 materials synthesized at different synthesis temperature and, thus, possessing different textural parameters (Table 2) are shown in Figure 13. The amount adsorbed is almost similar for SBA-15(100) and SBA-15(120), and is reduced for SBA-15(130) and SBA-15(150). The reduction in monolayer adsorption capacity n_m from SBA-15(100) to SBA-15(150) is in line with the reduced pore volume and surface area as compared to SBA-15(100). Such a behavior is expected since n_m is a function of the accessible pore volume (surface area). Moreover, it is well-known that the pore curvature decreases with increasing pore diameter. The reduced pore curvature affects the interaction between the neighboring cyt c molecules, which modifies the packing density of the cyt c molecules. This is reflected in the adsorption capacity of SBA-15(150). Hence, we surmise that the textural properties such as pore curvature, specific surface area, and specific pore volume are responsible for the differences in the amount of cyt c adsorption observed for C_{12}−MCM-41, C_{16}−MCM-41, and SBA-15 (Figure 13 (insert)).

(44) Munsch, S. Ph.D. Thesis, Kaiserslautern University of Technology, 2003.

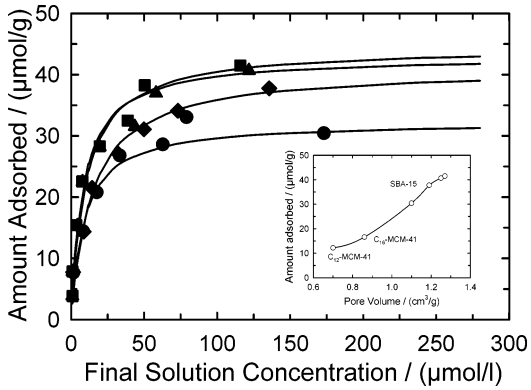

Figure 13. Cytochrome c adsorption isotherms at a pH of 9.6 on SBA-15 materials synthesized at different temperatures: (■) SBA-15(100), (▲) SBA-15(120), (◆) SBA-15(130), and (●) SBA-15(150). Insert: Adsorption capacity as a function of pore volume.

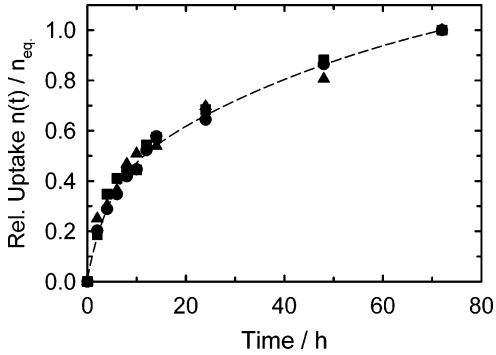

Figure 14. Relative uptake $n(t)/n_{eq.}$ ($n_{eq.}$ = amount adsorbed at thermodynamic equilibrium) versus time at pH = 6.5: (▲) C_{12}−MCM-41, (■) C_{16}−MCM-41, and (●) SBA-15.

Rate of Adsorption. The rate of adsorption expressed as $n(t)/n_{eq}$. ($n_{eq.}$ = amount adsorbed at thermodynamic equilibrium) of cyt c molecules on C_{12}−MCM-41, C_{16}−MCM-41, and SBA-15 versus time of adsorption is shown in Figure 14. The rate of adsorption is high up to 14 h (ca. 60% of the equilibrium value are reached) and is significantly reduced thereafter. All materials need at least 72 h to reach the equilibrium coverage of the adsorbent. While Deere et al.[34] have found that the adsorption is approximately 80% complete after 2 h for a starting concentration of 7.4 μmol/L, at an initial concentration of 80 μmol/L almost 50 h are needed to establish an adsorption that amounts to 80% of the equilibrium values. No major differences are found in

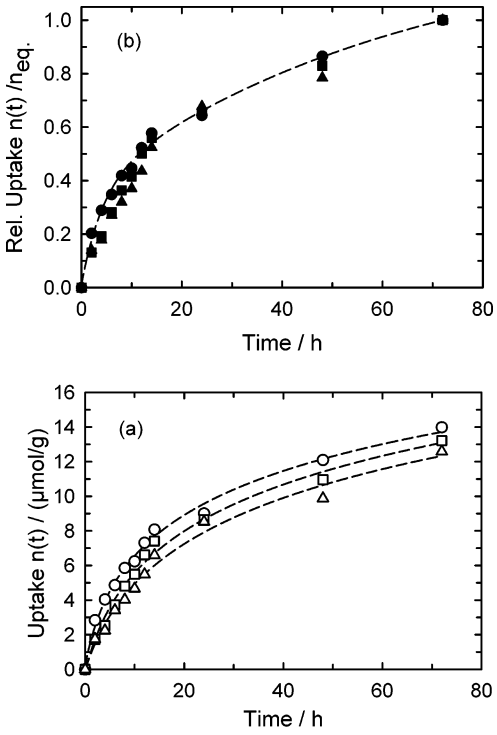

Figure 15. (a) Uptake $n(t)$ and (b) relative uptake $n(t)/n_{eq.}$ of SBA-15 materials as a function of time at pH = 6.5: (△) SBA-15 (unpressed powder), (□) SBA-15 (pressed at 43 MPa), and (○) SBA-15(107 MPa).

the rate of adsorption for the three materials used in the present study having rather large differences in pore diameter (Figure 14). It has to be concluded that the differences in pore diameter are affecting the adsorption kinetics only to a minor extent and that other factors such as the reconfiguration of the adsorbed cyt c layers have to be considered.[45] In this case, the adsorbed molecules undergo a reorientation to allow closer packing. It can be assumed that this process is very slow (maybe slower than the diffusion of cyt c) and, thus, will influence the adsorption kinetics.

For practical applications in adsorption columns, small beads or pellets are preferred since an adsorbent powder would result in a (not tolerable) large pressure drop. Therefore, the adsorption capacity and the rate of adsorption are reported for SBA-15 beads (prepared by pelletizing and sieving) exhibiting different textural properties as compared to the unpressed material (powder).[18] Figure 15a shows the uptake of cyt c on SBA-15 beads pressed at 43 and 107 MPa in comparison to the powder sample. The amount adsorbed is reduced which is in line with the reduction of the pore volume that was observed upon compression of the powder during the formation of the beads (Table 2). However, no differences in rate of adsorption (Figure 15b) are observed showing that the diffusion of cyt c in the beads is not hindered.

Conclusions

Different mesoporous materials (MCM-41 and SBA-15) with various pore diameters have been synthesized under different conditions and characterized by X-ray powder diffraction and nitrogen adsorption measurements. Adsorption of cytochrome c over these adsorbents has been studied from solutions with different pHs. It has been found that the amount of cyt c adsorbed on different adsorbents was significantly changed by adjusting the solution pH. The maximum loading of cyt c has been achieved near the isoelectric point of cyt c (pI = 9.8). This may due to the zero net charge of the cyt c molecule at this pH, and thus there is no electrostatic repulsion or attraction between the amino acid residues, resulting in a size reduction of the cyt c molecule. It has also been discovered that the amount of cyt c adsorption can be increased by the introduction of aluminum sites into the pure silica materials. The observed increase in adsorption capacity is probably a consequence of the strong electrostatic interaction between the negative charges on the aluminum sites and the positively charged amino acid residues on the surface of cytochrome c. The influence of pore diameter on the adsorption of cyt c has also been studied by using adsorbents with different pore diameter. It has been found that the amount adsorbed is mainly a function of the specific pore volume and that ca. 30% of the total pore volume is occupied by the protein. Furthermore, the rate of cyt c adsorption on the powder and the pellet form of the adsorbent has been studied. While the adsorption capacity is reduced upon bead formation (due to the reduction in specific pore volume), the rate of adsorption is mainly unchanged.

Acknowledgment. Financial support of this work by Deutsche Forschungsgemeinschaft (Ha2527/4-2) and Fonds der Chemischen Industrie is gratefully acknowledged.

Supporting Information Available: Figures with XRD powder patterns, nitrogen adsorption isotherms, and the pore size distributions of the pure silica and aluminum-containing MCM-41 and SBA-15 materials. This material is available free of charge via the Internet at http:// pubs.acs.org.

CM049718U

(45) Robeson, J. L.; Tilton, R. D. *Langmuir* **1996**, *12*, 6104.